Langmuir
Article
pubs.acs.org/Langmuir

Cholesterol Mediates Chitosan Activity on Phospholipid Monolayers and Langmuir−Blodgett Films

Felippe J. Pavinatto,[†] Cauê P. Pacholatti,[†] Érica A. Montanha,[†] Luciano Caseli,[‡] Heurison S. Silva,[†] Paulo B. Miranda,[†] Tapani Viitala,[§] and Osvaldo N. Oliveira Jr.*[,†]

[†]*Instituto de Física de São Carlos, Universidade de São Paulo, São Carlos, SP, Brasil,* [‡]*Departamento de Ciências Exatas e da Terra, Universidade Federal de São Paulo, Diadema, SP, Brasil, and* [§]*KSV Instruments, Hötlääämötie, 7, 00380, Helsinki, Finland*

Received March 23, 2009. Revised Manuscript Received June 8, 2009

The polysaccharide chitosan has been largely used in many biological applications as a fat and cholesterol reducer, bactericide agent, and wound healing material. While the efficacy for some of such uses is proven, little is known about the molecular-level interactions involved in these applications. In this study, we employ mixed Langmuir and Langmuir−Blodgett (LB) films of negatively charged dimyristoyl phosphatidic acid (DMPA) and cholesterol as cell membrane models to investigate the role of cholesterol in the molecular-level action of chitosan. Chitosan does not remove cholesterol from the monolayer. The interaction with chitosan tends to expand the DMPA monolayer due to its interpenetration within the film. On the other hand, cholesterol induces condensation of the DMPA monolayer. The competing effects cause the surface pressure isotherms of mixed DMPA−cholesterol films on a chitosan subphase to be unaffected by the cholesterol mole fraction, due to distinct degrees of chitosan penetration into the film in the presence of cholesterol. By combining polarization-modulated infrared reflection absorption spectroscopy (PM-IRRAS) and sum-frequency generation spectroscopy (SFG), we showed that chitosan induces order into negatively charged phospholipid layers, whereas the opposite occurs for cholesterol. In conclusion, chitosan has its penetration in the film modulated by cholesterol, and electrostatic interactions with negatively charged phospholipids, such as DMPA, are crucial for the action of chitosan.

Introduction

Interaction with biomembranes is essential for the action of biologically relevant molecules, including pharmaceutical drugs,[1−3] peptides,[4−6] proteins,[7−10] and polysaccharides such as chitosan.[11,12] The latter is a natural polysaccharide obtained from deacetylation of chitin, which has been used in various biological applications, e.g., as a fat reducer,[13] bactericide,[14,15] dressing and scaffolds for wound healing,[16] and in drugs and gene delivery.[17,18] It is biocompatible and biodegradable and displays low cytotoxicity.[19] The possible coupling with living cells has motivated studies of chitosan incorporated in model plasmatic membranes, where molecular-level information can be obtained. The use of liposomes,[20−25] Langmuir monolayers, and Langmuir−Blodgett (LB) films[11,12,26−28] as biomembrane models has become popular in view of the complexity of in vivo systems that make it impossible to distinguish between effects from the many components in a membrane. In spite of the simplifications adopted in these models, their usefulness has been demonstrated in cases where a clear correlation with physiological action could be established. By way of illustration, the ability of chitosan in removing the protein β-lactoglobulin from whey[28] has been related to sequestering of the protein from a monolayer of

*Corresponding author. Phone/Fax: 55 16 3373-9825.

(1) Caetano, W.; Ferreira, M.; Tabak, M.; Sanchez, M. I. M.; Oliveira, O. N. Jr.; Kruga, P.; Schalke, M.; Losche, M. *Biophys. Chem.* **2001**, *91*, 21–35.
(2) Chimote, G.; Banerjee, R. *Coll. Surf. B* **2008**, *62*, 258–264.
(3) Suwalsky, M.; Villena, F.; Sotomayor, C. P.; Bolognin, S.; Zatta, P. *Biophys. Chem.* **2008**, *135*, 7–13.
(4) Huo, Q.; Sui, G. D.; Zheng, Y.; Kele, P.; Leblanc, R. M.; Hasegawa, T.; Nishijo, J.; Umemura, J. *Chem.−Eur. J.* **2001**, *22*, 4796–4804.
(5) Lourenzoni, M. R.; Namba, A.; Caseli, L.; Degreve, L.; Zaniquelli, M. E. D. *J. Phys. Chem. B* **2007**, *111*, 1351–1360.
(6) Tae, G.; Yang, H.; Shin, K.; Satija, S. K.; Torikai, N. *J. Peptide Sci.* **2008**, *14*, 461–468.
(7) Thakur, G.; Wang, C; Leblanc, R. M. *Langmuir* **2008**, *24*, 4888–4893.
(8) Wang, C.; Micic, M.; Ensor, M.; Daunert, S.; Leblanc, R. M. *J. Phys. Chem. B* **2008**, *112*, 4146–4151.
(9) Caseli, L.; Pavinatto, F. J.; Nobre, T. M.; Zaniquelli, M. E. D.; Viitala, T.; Oliveira, O. N. Jr. *Langmuir* **2008**, *24*, 4150–4156.
(10) Caseli, L.; Moraes, M. L.; Zucolotto, V.; Ferreira, M.; Nobre, T. M.; Zaniquelli, M. E. D.; Rodrigues, U. P.; Oliveira, O. N. Jr. *Langmuir* **2006**, *22*, 8501–8508.
(11) Pavinatto, F. J.; Pavinatto, A.; Caseli, L.; Dos Santos, D. S. Jr.; Nobre, T. M.; Zaniquelli, M. E. D.; Oliveira, O. N. Jr. *Biomacromolecules* **2007**, *8*, 1633–1640.
(12) Pavinatto, F. J.; Caseli, L.; Pavinatto, A.; Dos Santos, D. S. Jr.; Nobre, T. M.; Zaniquelli, M. E. D.; Silva, H. S.; Miranda, P. B.; Oliveira, O. N. Jr. *Langmuir* **2007**, *23*, 7666–7671.
(13) Park, G. Y.; Mun, S.; Park, Y.; Rhee, S.; Decker, E. A.; Weiss, J.; McClements, D. J.; Park, Y. *Food Chem.* **2007**, *104*, 761–767.
(14) Rabea, E. I.; Badawy, M. E-T.; Stevens, C. V.; Smagghe, G.; Steurbaut, W. *Biomacromolecules* **2003**, *4*, 1457–1465.
(15) Liu, H.; Du, Y.; Wang, X.; Su, L. *Int. J. Food Microb.* **2004**, *95*, 147–155.
(16) Kumar, M. N. V. R.; Muzzarelli, R. A. A.; Muzzarelli, C.; Sashiwa, H.; Domb, A. J. *Chem. Rev.* **2004**, *104*, 6017–6084.
(17) Agnihotri, S.; Mallikarjuna, N. N.; Aminabhavi, T. M. *J. Controlled Release* **2004**, *100*, 5–28.
(18) Kima, T.-H.; Jianga, H.-L.; Jerea, D.; Parka, I.-K.; Chob, M.-H.; Nahc, J.-W.; Choia, Y.-J.; Akaiked, T.; Cho, C.-S. *Prog. Polym. Sci.* **2007**, *32*, 726–753.
(19) Rinaudo, M. *Prog. Polym. Sci.* **2006**, *31*, 603–632.
(20) Fang, N.; Chen, V.; Mao, H. Q.; Leong, K. W. *Biomacromolecules* **2001**, *2*, 1161–1168.
(21) Fang, N.; Chan, V. *Biomacromolecules* **2003**, *4*, 581–588.
(22) Fang, N.; Chan, V. *Biomacromolecules* **2003**, *4*, 1596–1604.
(23) Quemeneur, F.; Rammal, A.; Rinaudo, M.; Pepin-Donat, B. *Biomacromolecules* **2007**, *8*, 2512–2520.
(24) Quemeneur, F.; Rinaudo, M.; Pepin-Donat, B. *Biomacromolecules* **2008**, *9*, 396–402.
(25) Quemeneur, F.; Rinaudo, M.; Pepin-Donat, B. *Biomacromolecules* **2008**, *9*, 2237–2243.
(26) Pavinatto, F. J.; Dos Santos, D. S. Jr.; Oliveira, O. N. Jr. *Polímeros: Ciência Tecnol.* **2005**, *15*, 91–94.
(27) Parra-Barraza, H.; Burboa, M. G.; Sanchez-Vasquez, M.; Juarez, J.; Goycoolea, F. M.; Valdez, M. A. *Biomacromolecules* **2005**, *6*, 2416–2427.
(28) Wydro, P.; Krajewska, B.; Hac-Wydro, K. *Biomacromolecules* **2007**, *8*, 2611–2617.

negatively charged phospholipids.[9] Experimental evidence was obtained from surface pressure isotherms, polarization modulated infrared reflection absorption spectroscopy (PM-IRRAS) and fluorescence spectroscopy, proving that chitosan complexes to β-lactoglobulin adsorbed on a phospholipid monolayer, then removing it from the interface.[9]

Among the many applications of chitosan, one of the most widespread and proven is as a bactericide agent. However, the molecular-level mechanism of action is not known. It is thought that chitosan adsorbs on the bacterial cell surface,[14,15] increasing the permeability of the inner and outer membrane and disrupting bacterial cell membranes, with the release of cellular contents. This damage is probably caused by the electrostatic interaction between NH_3^+ groups of chitosan and phosphoryl groups of phospholipids in cell membranes. Side effects from the interaction between chitosan and cell membranes are also important, as one needs to know whether mutations occur when chitosan is employed in wound healing and in prostheses.[30,31] The interaction with the membrane can be mediated by cholesterol, as chitosan may induce the hypolipidemic mechanism when bound to lipoproteins associated with cholesterol (such as low density lipoprotein and high density lipoprotein). Therefore, learning about the interaction with cholesterol may help unveil the effects leading to the activity in wound healing and as a bactericide.

In this study, we build upon knowledge acquired in recent years on the interaction between chitosan and membrane models[11,12,20−28] to address the effects from adding cholesterol. Chitosan adsorbs onto phospholipid and cholesterol monolayers,[11,12,26−28] though it is not significantly surface active on its own under the conditions used in these papers. It causes monolayer expansion with a decrease in elasticity. Phospholipids with the zwitterionic choline as a polar group are frequently employed for mimicking biomembranes,[32−35] while negatively charged phospholipids are also of interest as they constitute up to 20% of cell membranes.[36] Here, we investigate the interaction between chitosan and cholesterol in pure and mixed Langmuir and Langmuir−Blodgett (LB) films with the negatively charged dimyristoyl phosphatidic acid (DMPA), because electrostatic interactions are known to be important for the chitosan action.[12,36,37] DMPA was chosen because its simple structure allows us to extrapolate the results to other negative phospholipids, in addition to allowing easy deposition as LB films. Significantly, studies on the interaction of cholesterol with negative lipids are still scarce,[36] with no reported work in Langmuir films. Of particular importance for the action of guest molecules in model membranes are the changes induced in packing, elasticity, and ordering of the membrane. In this context, a distinguishing feature of the present study is the combination of two methods capable of providing information on the ordering in Langmuir monolayers and LB films, namely PM-IRRAS, which is employed here for in situ analysis of monolayers at the air/water interface, and sum frequency generation (SFG) spectroscopy used to study deposited LB films.

Experimental Section

Dimyristoyl phosphatidic acid (DMPA), dipalmitoyl phosphatidyl choline (DPPC), and dipalmitoyl phosphatidyl glycerol (DPPG) were purchased from Avanti Polar Lipids, while cholesterol (3β-hydroxy-5-cholestene, 95%, GC) was acquired from Sigma Chemical Co, all being used as received. Chitosan was obtained from Galena (Brasil), with a degree of acetylation of 22% as determined by H^1 NMR spectroscopy. It was purified through dissolution in HCl medium, pH 3, then filtering and reprecipitation in a NaOH basic medium, pH 10. It had a molecular weight, M_n, of 113 kDa, with polydispersity index of 4.2 determined by size exclusion chromatography (SEC, Shimadzu) under the conditions given in ref 9.

Langmuir and Langmuir−Blodgett (LB) films were fabricated with a mini-KSV Langmuir trough housed in a class 10 000 clean room. The trough is equipped with a surface pressure sensor based on the Wilhelmy method and a Kelvin probe to measure surface potential. Aliquots of DMPA and cholesterol in chloroform (Mallinckrodt), 0.50−1.00 mg mL^{-1}, were spread on a Theorell−Stenhagen buffer subphase (NaOH, citric acid, boric acid, phosphoric acid, whose pH was adjusted to 3.0 with addition of HCl, 2 mol L^{-1}). Water for preparing the buffer solution was supplied by a Milli-RO coupled to a Milli-Q purification system from Millipore, with a resistivity of 18.2 MΩ cm and pH $\sim$ 6. The chitosan samples were dissolved in the buffer at concentrations between 0.05 and 0.50 mg mL^{-1} and employed as a subphase for DMPA and cholesterol monolayers. The ionic strength was fixed at 0.03 mol L^{-1}, at which chitosan adopts a random coil conformation.[39] Compression was performed using movable barriers with a relative speed of 5 $Å^2$ $molecule^{-1}$ min^{-1}. Surface pressure−area ($\pi-A$) and surface potential−area ($\Delta V-A$) isotherms were measured simultaneously at 23 $\pm$ 1 °C. From the $\pi-A$ isotherms, we calculated the surface compressional modulus C_s^{-1} (also referred to as the equilibrium in-plane elasticity[40]), using $C_s^{-1} = A(\partial\pi/\partial A)$, where A is the mean molecular area and π is the surface pressure.

Polarization-modulation infrared reflection absorption spectroscopy (PM-IRRAS) was performed using a KSV PMI550 instrument (KSV, Finland). The experimental setup used was similar to that described by Blaudez and co-workers.[41] The Langmuir trough is setup so that the light beam reaches the monolayer at a fixed incidence angle of 80°. The incoming light is continuously modulated between s- and p-polarization at a high frequency, which allows simultaneous measurement of the spectra for the two polarizations. The two channels processing the detected signal give the differential reflectivity spectrum $\Delta R = (R_p - R_s)/(R_p + R_s)$, where R_p and R_s are respectively the polarized reflectivities for parallel and perpendicular directions to the plane of incidence. Absorption from the parallel polarized light beam is sensitive mostly to vertically oriented dipoles, while the perpendicularly polarized beam is sensitive to those horizontally oriented. The difference spectrum thus provides information on oriented moieties, which is generally surface specific, since molecules in the subphase have random orientations. As the spectra are measured simultaneously and the IR spectrum is divided by the corresponding spectrum of the subphase, the effect of water vapor is largely reduced. In the angle used in this work, upward-oriented bands indicate a transition moment preferentially in the surface plane,

(29) Casal, E.; Montilla, A.; Roeno, F. J.; Olano, A.; Corzo, N. *J. Dairy Sci.* **2006**, *89*, 1384–1389.
(30) Khora, E.; Lim, L. Y. *Biomaterials* **2003**, *24*, 2339–2349.
(31) Di Martino, A.; Sittinger, M.; Risbud, M. V. *Biomaterials* **2005**, *26*, 5983–5990.
(32) Zheng, L.; McQuaw, C. M.; Ewing, A. G.; Winograd, N. *J. Am. Chem. Soc.* **2007**, *129*, 15730–15731.
(33) Bonn, M.; Roke, S.; Berg, O.; Juurlink, L. B. F.; Stamouli, A.; Muller, M. *J. Phys. Chem. B* **2004**, *108*, 19083–19085.
(34) McConnell, H. M.; Radhakrishnan, A. *Biochim. Biophys. Acta* **2003**, *1610*, 159–173.
(35) Coban, O.; Popov, J.; Burger, M.; Vobornik, D.; Johnston, L. J. *Biophys. J.* **2007**, *92*, 2842–2853.
(36) Pott, T.; Maillet, J.-C.; Dufourc, E. J. *Biophys. J.* **1995**, *69*, 1897–1908.
(37) Montilla, A.; Casal, E.; Moreno, F. J.; Belloque, J.; Olano, A.; Corzo, N. *Int. Dairy J.* **2007**, *17*, 459–464.
(38) Sogias, I. A.; Williams, A. C.; Khutoryanskiy, V. V. *Biomacromolecules* **2008**, *9*, 1837–1842.
(39) Tsaih, M. L.; Chen, R. H. *J. Appl. Polym. Sci.* **1999**, *73*, 2041–2050.
(40) *Interfacial Phenomena*, 2nd ed.; Davies, J. T., Rideal, E. K., Eds.; Academic Press: New York, 1963.
(41) Blaudez, D.; Buffeteau, T.; Cornut, J. C.; Desbat, B.; Escafren, N.; Pezolet, M.; Turlet, J. M. *Appl. Spectrosc.* **1993**, *47*, 869–874.

whereas downward-oriented bands indicate preferential orientation perpendicular to the surface.

The transfer of DMPA, cholesterol, or mixed DMPA−cholesterol, DMPA−chitosan, cholesterol−chitosan, and DMPA−cholesterol−chitosan monolayers onto solid supports was performed at a constant surface pressure of 40 mN m^{-1} and dipping speed of 5.0 mm min^{-1}, which rendered a transfer ratio close to unity and points to a uniform film deposition. For mixed DMPA−chitosan, cholesterol−chitosan, and DMPA−cholesterol−chitosan monolayers, the concentration of chitosan in the subphase was 0.20 mg mL^{-1}. Substrates were AT-cut quartz crystal coated with Au (Stanford Research Systems Inc.), with fundamental frequency of ca. 5 MHz for nanogravimetry measurements (QCM quartz crystal microbalance), and infrared-grade fused silica for sum-frequency generation spectroscopy (SFG). Only one-layer LB films were produced.

SFG was used to study the structuring of DMPA and cholesterol in Langmuir−Blodgett films. This method is sensitive to conformation and molecular ordering, according to selection rules of the nonlinear optical susceptibility at interfaces. A detailed theory of SFG is available in the literature,[42−44] and only a brief description is given here. The SFG signal is obtained by impinging two laser beams with frequencies ω_{vis} and ω_{IR} that overlap at an interface, thus generating an output at frequency $\omega_{SFG} = \omega_{vis} + \omega_{IR}$. Because the signal is proportional to the square of the nonlinear susceptibility χ_s^2 ($\omega_{SFG} = \omega_{vis} + \omega_{IR}$), it will be zero within the electric dipole approximation in any media with inversion symmetry. One may therefore perform nonlinear spectroscopy at an interface by tuning ω_{IR}, with a surface vibrational spectrum being obtained by the enhancement of χ^2 as ω_{IR} coincides with a vibrational resonance. For the DMPA-containing films investigated in this paper, ordering is associated with the conformation of alkyl chains by analyzing the CH stretch region of the SFG spectra.[45,46] The SFG spectrometer was purchased from Ekspla (Lithuania) and consists of a pulsed Nd^{3+}:YAG laser that provides a fundamental beam at 1064 nm (25 ps pulse duration, 20 Hz repetition rate), with a harmonic unit generating second and third harmonics (532 and 355 nm, respectively). The sample is excited by the visible beam with pulse energy of ca. 950 μJ, while the infrared (IR) beam is generated by an optical parametric amplifier and difference-frequency stage pumped by the third harmonic and fundamental beams. The IR beam is tunable from 1000 to 4000 cm^{-1} with pulse energy ~ 30−150 μJ. The spot sizes and incidence angles for the IR and visible beams are 0.50 mm, 55°, and 1.00 mm, 60°, respectively. The SFG signal is measured with a photomultiplier after spatial and spectral filtering, with data being collected for each scan with 100 shots data $point^{-1}$ in 3 cm^{-1} increments. All experiments were performed at 23 ± 1 °C.

Results and Discussion

The main thrust of the present work is in the analysis of how chitosan affects a model membrane represented by a phospholipid (DMPA) monolayer in the presence of cholesterol. The choice of a negatively charged phospholipid was based on previous knowledge that chitosan activity is strongly related to electrostatic interactions with the membrane. Such analysis requires a comparison with results from systems used as references. Accordingly, before discussing the effects from chitosan on mixed DMPA−cholesterol monolayers, a description is given of the main findings for neat DMPA monolayers, neat cholesterol, and mixed DMPA−cholesterol monolayers with no chitosan.

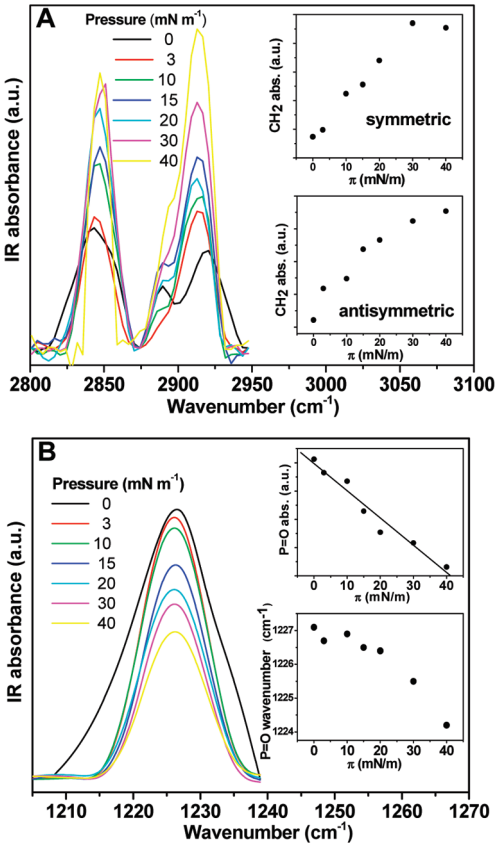

Figure 1. PM-IRRAS spectra for DMPA monolayer on Theorell buffer subphase (pH ~ 3.0) for several surface pressures for the (A) CH_2 and CH_3 and (B) P═O vibration regions. The insets show the change in band intensity with surface pressure.

Neat DMPA Monolayers. DMPA monolayers spread onto pure water or on a Theorell buffer solution, as performed here, have been characterized in a previous work.[12] Basically, the area per DMPA molecule is larger for the monolayer on the buffer than on pure water, which is attributed to the ion exchange between H^+ from the phosphate headgroup and cations in the buffer solution.[36] Since such data are available in the literature, they were omitted here. We discuss only the PM-IRRAS data, which—to our knowledge—have not been described before.

The PM-IRRAS spectra for the C−H stretching mode region, shown in Figure 1A, are dominated by strong bands at 2911−2918 and 2841−2848 cm^{-1}, assigned to the antisymmetric and symmetric CH_2 stretching vibrations, respectively. The shoulder at 2890 cm^{-1} is assigned to the symmetric stretch of CH_3 groups and has low resolution as in other phospholipid monolayers.[47] The band for CH_2 antisymmetric vibrations is slightly shifted to lower wavenumbers with increasing pressure, from 2918 cm^{-1} at 0 mN m^{-1} to 2911 cm^{-1} at 40 mN m^{-1}, while the band for symmetric vibrations is shifted to higher wavenumbers. This is probably due to the increased number of trans conformers along the lipid chains, which correlates with increasing order upon monolayer compression.[48] Another possible cause for the shift is nonhomogeneity and coexistence of fluid and gel phases.[49] Under the conditions employed here, the DMPA monolayer possesses a gaseous or gaseous-to-liquid state down to molecular areas as low as 70 $Å^2$. A liquid-expanded state is reached at molecular areas

(42) Zhuang, X.; Miranda, P. B.; Kim, D.; Shen, Y. R. *Phys. Rev. B* **1999**, *59*, 12632–12640.
(43) Shen, Y. R. *Surf. Sci.* **1994**, *299/300*, 551–562.
(44) Lambert, A. G.; Davies, P. B.; Neivandt, D. J. *Appl. Spectr. Rev.* **2005**, *40*, 103–145.
(45) Ma, G.; Allen, H. C. *Photochem. Photobiol.* **2006**, *82*, 1517–1529.
(46) Guyot-Sionnest, P.; Hunt, J.; Shen, Y. R. *Phys. Rev. Lett.* **1987**, *59*, 1597–1600.
(47) Bin, X. M.; Lipkowski, J. *J. Phys. Chem. B* **2006**, *110*, 26430–26441.
(48) Dicko, A.; Bourque, H.; Pezolet, M. *Chem. Phys. Lipids* **1998**, *96*, 125–139.
(49) Okamura, E.; Umemura, J.; Takenaka, T. *Biochim. Biophys. Acta* **1985**, *812*, 139–146.

lower than 70 Å^2, with a liquid-condensed phase being fully attained at 45 Å^2, for surface pressures higher than 4−5 mN m^{-1}. In this pressure range, the DMPA monolayer undergoes a first-order phase transition from the liquid-expanded to the liquid-condensed phase, with a plateau on the surface pressure−area isotherm.[12] Collapse occurs above 50 mN m^{-1}. The phase transition during monolayer compression may lead to microdomains, thus affecting orientation of DMPA chains at the air−water interface. The intensity of the symmetric and antisymmetric bands increases with surface pressure owing to the higher DMPA surface density, as shown in the insets of Figure 1A. The intensity of the symmetric band levels off at high surface pressures because of the low monolayer compressibility, i.e., large changes in pressure correspond to a slight increase in surface density.

The spectra in the P═O stretch region shown in Figure 1B have a band centered at 1226 cm^{-1} for all pressures. The band intensity for this antisymmetric P═O stretch decreases with the surface pressure, suggesting changes in orientation of the headgroup during compression. The phosphate group is thought to be involved in intermolecular hydrogen bonding with lateral glycerol moieties for DPPG films.[50] The energy for this DMPA band is higher than for DPPG (1223 cm^{-1}),[48] which can indicate higher degree of hydration of DMPA phosphate group and/or stronger hydrogen bonds with neighboring molecules at the air−water interface. It is also possible that the P═O groups located beneath the air−water interface could be screened by the dense packing of hydrophobic chains at the air−water interface, which may be enhanced with monolayer packing.

Effects from Chitosan on Neat DMPA Monolayers. Chitosan on its own is not surface active, and compression of its solution surface yields surface pressures less than 1.0 mN m^{-1}.[11] This means that chitosan does not form Gibbs monolayers for the range of concentrations employed here (up to 0.50 mg mL^{-1}). Chitosan has nevertheless a lipid-induced surface activity when a monolayer is present at the air−water interface. It causes expansion in monolayers of phospholipids,[11,12] fatty acids,[27,28] and cholesterol.[26,27] For DMPA, in particular, expansion saturates for a chitosan concentration of 0.20 mg mL^{-1} in the subphase, in addition to decreasing the monolayer elasticity and increasing the surface potential. Chitosan forms a subsurface below the lipid polar groups and may penetrate in the hydrophobic region of the film, in an interaction that may involve a combination of electrostatic, ion−dipole, and hydrophobic forces.[11,12]

In the PM-IRRAS spectra with chitosan in the subphase, the bands for the CH_3 symmetric stretching bands (shoulder) are more clearly seen than for neat DMPA, as indicated in Figure 2. This is consistent with the enhanced alignment of alkyl chains induced by chitosan observed with SFG measurements.[12] As CH_2 bands are less intense than for pure DMPA, probably chitosan interpenetrated among the alkyl tails, decreasing the surface density of phospholipid. Also, CH_2 antisymmetric stretching is strongly shifted to lower wavenumbers with increasing pressure, e.g. with the band being centered at 2908 cm^{-1} at 40 mN m^{-1}. Furthermore, the CH_2 symmetric stretching shifted from 2847 to 2850 cm^{-1}, pointing to an increase in order upon incorporation of chitosan. This is confirmed by the appearance of the shoulder at 2895 cm^{-1}, assigned to CH_3 symmetric stretch vibrations.

As one may expect, incorporation of chitosan has a strong effect on the headgroup region of the DMPA monolayer, which is here analyzed by considering the PM-IRRAS spectra for the

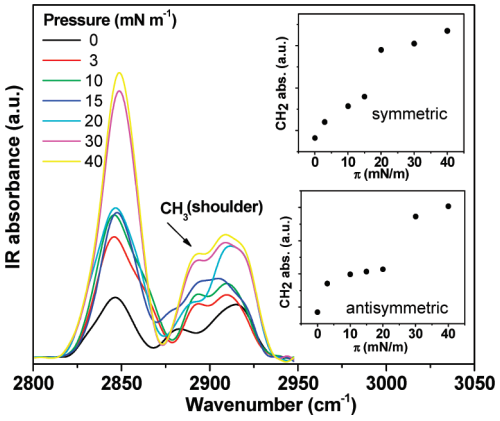

Figure 2. PM-IRRAS spectra for DMPA monolayer on 0.20 mg mL^{-1} chitosan dissolved in Theorell buffer (pH ∼ 3.0) for several surface pressures. The insets on the right show the evolution of band intensities for the two main bands.

phosphate and amine bands (Figure 3A and B). Both the intensity and energy for the P═O stretch band at 1225−1270 cm^{-1} decrease with increasing pressures, while for neat DMPA the intensity decreased but the energy remained constant. At high surface pressures (30 and 40 mN m^{-1}), the P═O bands seem to have two contributions, which may be ascribed to the interaction between amine groups and chitosan.

Therefore, the interaction between chitosan and phosphate groups appears to become stronger upon compression. The spectra in the amine band region, shown in Figure 3B, display bands at 1535 and 1556−1560 cm^{-1}, corresponding to N−H deformation. The band at 1535 cm^{-1} is due to protonated amines of chitosan ($-NH_3^+$ symmetric bend),[51] and the one at ∼1560 is the NH bend of the acetylated glucosamine residues (−NH−CO−, amide II band).[52,53] The band intensities decrease above 20 mN m^{-1}, along with a shift to lower wavenumbers for the amide II band. At 20 mN m^{-1}, the close packing of DMPA monolayer starts affecting more markedly the interaction between chitosan and the head groups. In fact, at this surface pressure, the liquid-condensed state has already been reached,[12] and this represents a limit for the amine groups of chitosan to be exposed at the interface.

Effects from Chitosan upon Neat Cholesterol Monolayers. Monolayers of cholesterol over chitosan-containing subphases have already been reported in the literature.[26,27] Nevertheless, because slight changes may occur depending on the chitosan samples used, e.g. on the degree of deacetylation and molecular weight, we obtained the surface characterization of this system, in order to make a direct comparison with mixed phospholipid monolayers. The results of surface pressure and surface potential isotherms were consistent with the literature for cholesterol[54] and chitosan-containing cholesterol monolayers[26,27] and are omitted. Overall, the presence of cholesterol at the interface induces adsorption of chitosan, causing expansion of surface pressure as well as surface potential isotherms. Both the surface potential and the degree of expansion increase with chitosan concentration, but a saturation of this effect was

(50) Zhang, Y. P.; Lewis, R. N. A. H.; McElhaney, R. N. *Biophys. J.* **1997**, *72*, 779–793.

(51) Lawrie, G.; Keen, I.; Drew, B.; Chandler-Temple, A.; Rintoul, L.; Fredericks, P.; Grndahl, L. *Biomacromolecules* **2007**, *8*, 2533–2541.

(52) Shigemasa, Y.; Matsuura, H.; Sashiwa, H.; Saimoto, H. *Int. J. Biol. Macromol.* **1996**, *18*, 237–242.

(53) Dong, Y.; Xu, C.; Wang, J.; Wang, M.; Wu, Y.; Ruan, Y. *Sci. Chin. (Ser. B)* **2001**, *44*, 216–224.

(54) Dynarowicz-Latka, P.; Hac-Wydro, K. *Colloids Surf. B: Biointerfaces* **2004**, *37*, 21–25.

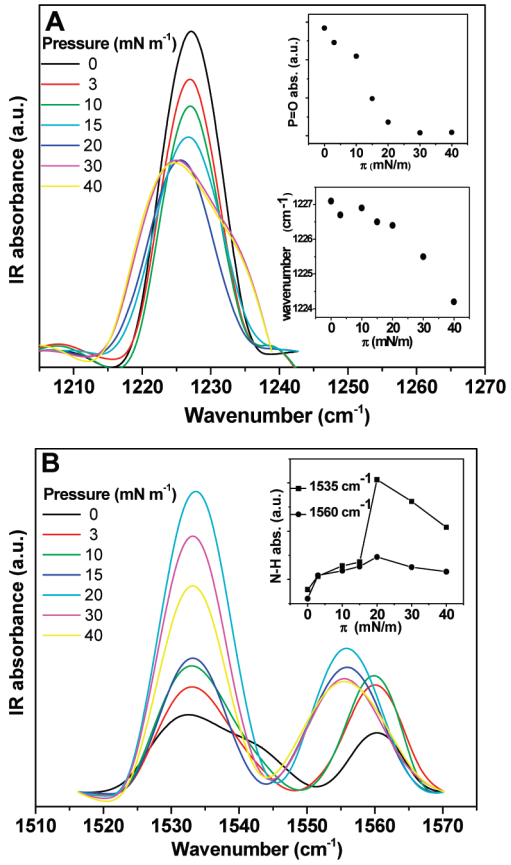

Figure 3. PM-IRRAS spectra for DMPA monolayer on 0.20 mg mL^{-1} chitosan dissolved in Theorell buffer (pH ~ 3.0) for several surface pressures, where the regions for phosphate bands (A) and amine bands (B) are shown. The insets on the right of Figure 3A show the band intensity and position. The inset of Figure 3B depicts the evolution of band intensities for the two main bands.

observed above 0.30 mg mL^{-1} (subsidiary experiments, results not shown). This saturation was reported in a previous study from our group,[26] but at a different concentration, ca. 0.10 mg mL^{-1}, as the chitosan sample had a different molecular weight and polydispersity index. These findings may be important for practical applications of chitosan, as the chemical structure of chitosan used in formulations, such as medicines, have noticeable influence on the effects over biological systems. For instance, an optimum dosage and physiological effect can be estimated for a specific sample of chitosan.

Cholesterol monolayers with incorporated chitosan are more compressible than a pure cholesterol monolayer (for isotherms, see the Supporting Information). For a chitosan concentration up to 0.30 mg mL^{-1}, the compressional modulus decreases with chitosan concentration whereas the mean molecular area increases, for a fixed pressure of 30 mN m^{-1}. This is common for macromolecules interacting with lipid monolayers, as reported for several proteins.[10] As a "soft" material, chitosan makes the film more flexible, decreasing the original rigidity of pure lipid monolayers, able to pack in regular patterns.

Figure 4 shows that chitosan has little effect on the spectroscopic properties of cholesterol monolayers. At $\pi = 30$ mN m^{-1}, the band at 2928 cm^{-1} remains at the same position, and the amine bands have intensity practically unchanged for increasing surface pressures (results not shown). Shifts in the spectra are negligible, indicating that interaction of chitosan with cholesterol is independent of surface packing. The inset shows the OH

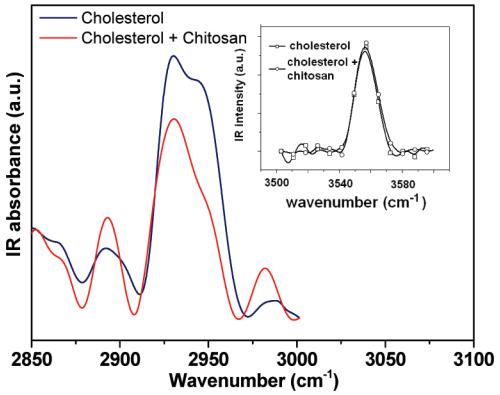

Figure 4. PM-IRRAS spectra for cholesterol Langmuir monolayer on Theorell buffer (pH ~ 3.0) in the presence and absence of 0.20 mg mL^{-1} chitosan in two spectral regions: 2800−3000 cm^{-1} for CH_2 stretching and 3500−3600 cm^{-1} for OH stretching (inset). The surface pressure was 30 mN m^{-1}.

stretching band at 3556 cm^{-1}, which is not affected by chitosan either. Thus, chitosan does cause cholesterol monolayers to expand,[26] but its effect on cholesterol head groups is small compared to that on DMPA.

DMPA−Cholesterol Mixed Monolayers. We now turn to a more sophisticated membrane model, with chitosan interacting with both DMPA and cholesterol in the same monolayer. To our knowledge, mixed DMPA−cholesterol monolayers have not been reported, and we then analyze them first before adding chitosan.

Figure 5A shows that neat DMPA has a larger area per molecule than cholesterol for the subphase conditions used, which is ascribed not only to their different structures but also to the presence of ions in the aqueous subphase. For DMPA on pure water, the extrapolated area per molecule is approximately 40 $Å^2$, but on the Theorell buffer the area is considerably larger because DMPA is sensitive to ions in the subphase that can interexchange with H^+.[36,55] Cholesterol also causes the DMPA monolayer to become more rigid, i.e. the compressibility modulus increases. For instance, at 30 mN m^{-1}, a pure DMPA monolayer has C_s^{-1} of 105 mN m^{-1}, which increases to 204 mN m^{-1} for a mixture with 50% of cholesterol. As expected, isotherms for mixed films are comprised between curves for the neat compounds. However, evidence for a nonideal mixture of cholesterol and DMPA is readily seen, which will be discussed later. The isotherms in Figure 5B show that at low molecular areas the surface potential is roughly the same for all DMPA-containing monolayers, regardless of the cholesterol quantity. The main effect of cholesterol appears in condensing the monolayer, and therefore, the surface potential isotherms at large areas are shifted to lower molecular areas as the amount of cholesterol increases. The positive surface potential at large areas of a pure DMPA monolayer on the Theorell buffer—in contrast to the expected negative surface potential arising from the contribution of the double-layer—means that the buffer causes DMPA molecules to be charged to a lesser extent than on pure water.

According to Goodrich[56] and Gaines,[57] an ideal mixture must follow the additivity rule, according to which the molecular area of the mixed monolayer (A_{12}) should be given by the molar average of its components, i.e.:

$$A_{12} = X_1A_1 + X_2A_2$$

(55) Ahuja, R. C.; Maack, J.; Tachibana, H. *J. Phys. Chem.* **1995**, *22*, 9221–9229.
(56) Goodrich, F. C. *Angew. Chem.—Int. Ed.* **1957**, *69*, 536–536.
(57) Gaines, G. L. *J. Colloid Interface Sci.* **1966**, *21*, 315–319.

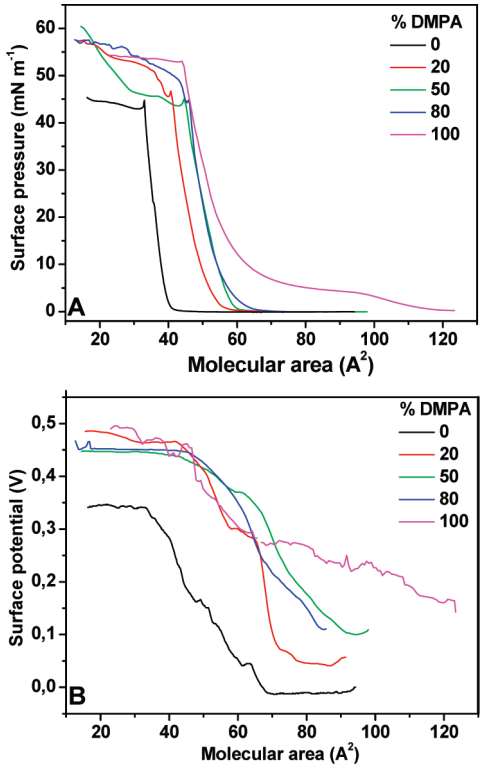

Figure 5. Surface pressure−area (A) and surface potential−area (B) isotherms for mixed DMPA−cholesterol monolayers on a Theorell buffer subphase, for various mole percents of DMPA. The area per molecule was calculated assuming that molecules of both DMPA and cholesterol remain at the interface, and therefore, it is not an area per phospholipid molecule. The surface pressure isotherm for the neat DMPA monolayer is slightly different from that of Figure 1 in ref 12, as the latter was obtained with 10^{-3} mol L^{-1} HCl subphase, instead of on Theorell buffer as it was wrongly informed in ref 12.

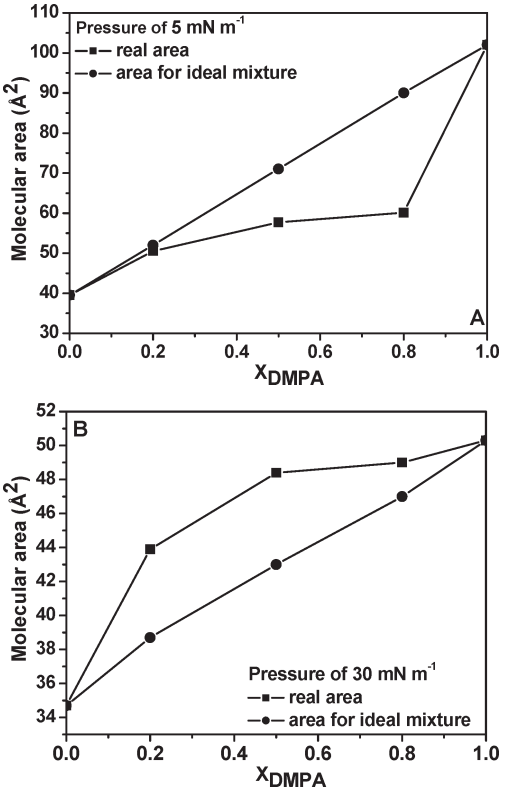

Figure 6. Real (measured) and ideal (calculated) average area per molecule for DMPA−cholesterol mixed monolayers on Theorell buffer subphases, for various mole percents of DMPA: at (A) 5 and (B) 30 mN m^{-1}.

where A_1 and A_2 are the areas per molecule for each component separately and X_1 and X_2 are molar fractions of each component in the mixture.

Figure 6A shows that at a low pressure there is a negative deviation from the ideal straight line for A_{12}, pointing to a condensing effect induced by cholesterol, and a negative excess of free energy (ΔG_{mix}) that makes the monolayer more stable.[56,58] This finding is consistent with the literature, i.e. an expanded monolayer is generally condensed by cholesterol due to a reduced hydrocarbon chain mobility.[59] The chain fluidity is reduced because sterol groups of cholesterol interact through van der Waals forces with the phospholipid hydrocarbon chains, thus disrupting the cooperative movements of the alkyl chains and increasing their orientational order. This has been reported for zwitterionic lipids such as cholines[59,60] and ethanolamines.[61] However, at high surface pressures (e.g., 30 mN m^{-1}), a positive deviation appeared (Figure 6B) indicating an expanding effect caused by cholesterol. Though less common, expansion induced by cholesterol has also been observed.[62−64] Zhai et al.[62] reported a positive deviation for ceramide−cholesterol mixed monolayers at high surface pressures. Wu et al.[63] mentioned that when charged groups are present, repulsion between groups can be enhanced by cholesterol, and expansion can occur. Korchowiec et al.[64] showed that cholesterol may expand even monolayers of zwitterionic phospholipids if the proportion of cholesterol was higher than 50%.

Our results therefore point to an expansion of the DMPA monolayer at a packing state comparable to that of a biological membrane (i.e., at ca. 30 mN m^{-1}),[65] which should be ascribed to increased repulsion among DMPA polar groups caused by an increase in the degree of dissociation induced by cholesterol. An expansion at high surface pressures was also observed for DMPA−cholesterol mixed monolayers on pure water, at which the condensed areas for both lipids coincide (ca. 40 Å^2) (results not shown). The same applied to cholesterol mixtures with the negatively charged dipalmitoyl phosphatidyl glycerol (DPPG), but not for DPPC, consistent with the hypothesis of a charge-dependent phenomenon (see the Supporting Information).

With regard to the PM-IRRAS spectra, a comparison between Figures 7A and 1A points to cholesterol increasing the difference in relative intensity of the CH_2 antisymmetric and symmetric bands, with the shoulder at 2889 cm^{-1} disappearing in the presence of cholesterol. The former may be due to a contribution from cholesterol to the PM-IRRAS spectrum, while the latter is an indication of disorder induced by cholesterol, which expands DMPA monolayers at high surface pressures.

(58) Bacon, K. J.; Barnes, G. T. *J. Colloid Interface Sci.* **1978**, *67*, 70–77.
(59) Ohe, C.; Sasaki, T.; Noi, M.; Goto, Y.; Itoh, K. *Anal. Bioanal. Chem.* **2007**, *388*, 73–79.
(60) Kim, Y. H.; Tero, R.; Takizawa, M.; Urisu, T. *Jpn. J. Appl. Phys.* **2004**, *43*, 3860–3864.
(61) Chapman, D.; Owens, N. F.; Phillips, M. C.; Walker, D. A. *Biochim. Biophys. Acta* **1969**, *3*, 458–465.
(62) Zhai, X. H.; Li, X. M.; Momsen, M. M.; Brockman, H. L.; Brown, R. E. *Biophys. J.* **2006**, *91*, 2490–2500.
(63) Wu, J. C.; Lin, T. L.; Yang, C. P.; Jeng, U. S.; Lee, H. Y.; Shih, M. C. *Colloid Surf. A−Physicochem. Eng. Asp.* **2006**, *284−285*, 103–108.
(64) Korchowiec, B.; Paluch, M.; Corvis, Y.; Rogalska, E. *Chem. Phys. Lipids* **2006**, *144*, 127–136.
(65) Marsh, D. *Biochim. Biophys. Acta* **1996**, *1286*, 183–223.

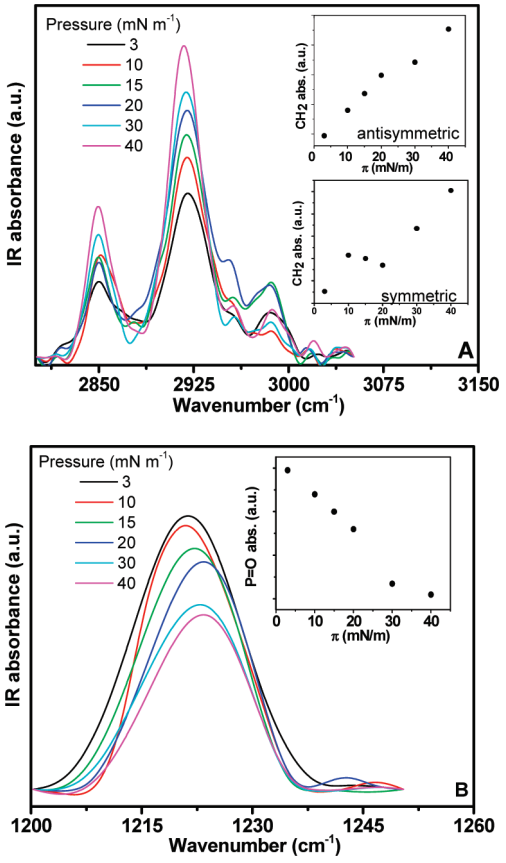

Figure 7. PM-IRRAS spectra for mixed DMPA−cholesterol monolayer (1:1 in moles) on Theorell buffer (pH ~ 3.0) for several surface pressures: region for (A) CH_2 vibrations and (B) the phosphate band. The insets on the right show the surface pressure dependence for the band intensities.

Cholesterol is reported to enhance the hydration of a mixed layer with DMPC and increase gauche conformations.[47] Our data indicate a shift in the phosphate band to lower frequencies, which should be associated not only with monolayer expansion, but also with hydrogen bonds involving surface water molecules with DMPA phosphate groups, which is facilitated with a more expanded monolayer. The band for the OH stretching in cholesterol is again unchanged (not shown). These results confirm that cholesterol causes expansion of DMPA monolayer, affecting the phosphate dissociation.

Effects from Chitosan on DMPA−Cholesterol Mixed Monolayers. Figure 8 shows the effect of chitosan on mixed monolayers of DMPA and cholesterol. It should be noted that the chitosan concentration used in the subphase was 0.20 mg mL^{-1}, which corresponds to the saturation concentration on DMPA monolayers.[12] Surprisingly, regardless of the cholesterol composition the mixed DMPA−cholesterol monolayers spread onto chitosan-containing subphases exhibited almost the same isotherms as for pure DMPA film. In other words, the expansion induced by chitosan in the subphase is independent of the cholesterol concentration. It may be recalled that in the absence of chitosan cholesterol molecules occupied smaller areas than DMPA; hence, upon increasing the cholesterol concentration, the area per molecule should decrease. However, the surface pressure isotherms in Figure 8A suggest that cholesterol now occupied the same areas as a DMPA molecule. Apparently, electrostatic interactions between DMPA polar groups and chitosan protonated amine groups determine the shape of the isotherms. This is

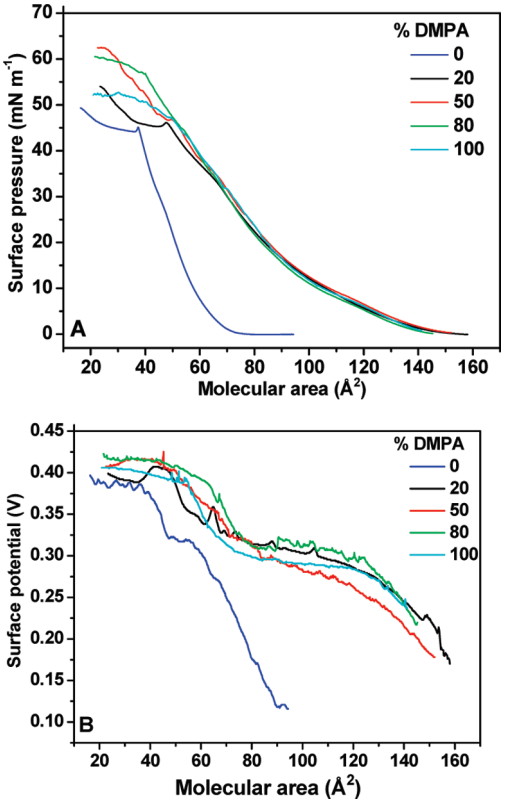

Figure 8. Surface pressure−area (A) and surface potential−area (B) isotherms for mixed DMPA−cholesterol monolayers on chitosan (0.20 mg mL^{-1}) subphase. The percentage of DMPA in moles is shown in the insert.

true even with DMPA being partly protonated in the pH used owing to exchange of counterions, whereby H^+ from phosphate head groups are replaced by NH_3^+ from chitosan.

Even though one could think of the role of cholesterol as apparently inert, the results for the mixed films with chitosan can only be understood if cholesterol modulates either the amount of chitosan that penetrates in the DMPA monolayer or the repulsion between phospholipid head groups. The coincidence of all curves from mixed films with that from a DMPA monolayer on a chitosan subphase may be indicative of a fixed number of protonated amines from chitosan that adsorbs at the interface. Then, regardless of the decrease in number of DMPA molecules, the pressure changes were negligible. Another possibility is the penetration of chitosan moieties to interact with hydrophobic groups of the phospholipid. Because replacing some DMPA molecules by cholesterol expands the monolayer, the area available at the air−water interface can be occupied by chitosan moieties. This hypothesis is consistent with the SFG data (see later) that pointed to an increased order caused by chitosan. Therefore, 20% of DMPA seemed to be sufficient to provide this effect. The expansion of mixed DMPA−cholesterol films induced by chitosan may not be ascribed to a possible tilting of cholesterol molecules due to chitosan adsorption, because the surface potential for pure DMPA monolayers over a chitosan-containing subphase is not affected by adding cholesterol (Figure 8B). Also, we believe the increased repulsion between head groups of DMPA is of minor importance since it would be accompanied by changes in the degree of dissociation of the phosphate acid groups. Such changes would affect the electric double-layer contribution to the surface potential,[66] which was not observed in the experimental results.

(66) Oliveira, O. N. Jr.; Taylor, D. M.; Lewis, T. J.; Salvagno, S.; Stirling, C. J. M. *J. Chem. Soc.: Faraday Trans.* **1989**, *85*, 1009–1018.

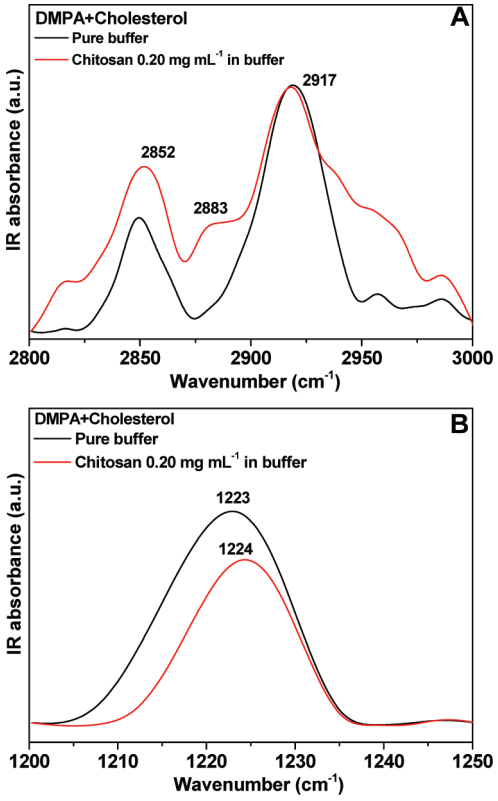

Figure 9. Comparison for PM-IRRAS spectra for the mixed DMPA−cholesterol monolayer (1:1 in moles) on Theorell buffer (pH ∼ 3.0) and on chitosan (0.20 mg mL^{-1}) for a surface pressure of 30 mN m^{-1}: region for (A) CH_2 vibrations and (B) the phosphate band.

The incorporation of chitosan to the mixed DMPA−cholesterol monolayers does not shift the band assigned to C−H vibration, but the CH_3 band appears at 2883 cm^{-1} in Figure 9A, an indication of increased order, which will be supported by SFG data to be presented later on. From Figure 9B, it is seen that the phosphate band for a fixed pressure of 30 mN m^{-1} is displaced slightly to higher wavenumbers in the presence of chitosan. The amine bands in Figure 10 have their intensity increased with the surface pressure. Interestingly, the intensity of the $-NH_3^+$ band at 1520 cm^{-1} reached a maximum at 15 mN m^{-1} and decreased upon further compression, probably owing to reorientation of this group during compression.

In summary, the effect from chitosan on mixed films should be attributed to the strong electrostatic interactions between the positively charged chitosan and the partially negatively charged DMPA, which dominate the surface properties. Dipole−charge interactions between hydroxyl groups of cholesterol and DMPA are replaced by stronger electrostatic interactions between DMPA and chitosan. Hence, the effect from cholesterol is only in promoting monolayer expansion (at high surface pressures) that enhances DMPA ionization, favoring its electrostatic interaction with chitosan. The primary interaction between chitosan and cholesterol should be through hydrogen bonds among hydroxyls and amines.[27] As for the penetration into the monolayer, Wydro et al. suggested that chitosan molecules may get accommodated in monolayers via hydrophobic interactions,[28] which is consistent with chitosan gel formation in aqueous solutions.[67] The interaction is believed to occur in two steps:[28] In

(67) Garcia, R. B.; Da Silva, D. L. P.; Costa, M.; Raffin, F. N.; Ruiz, N. M. D. *Quim. Nova* **2008**, *31*, 486–492.

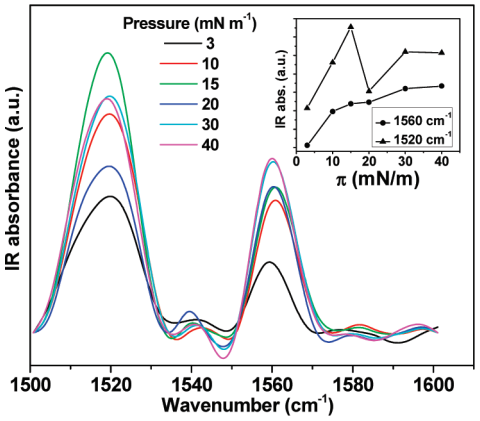

Figure 10. PM-IRRAS spectra in the amine bands region for mixed DMPA−cholesterol monolayer (1:1 in mol) on chitosan-containing (0.20 mg mL^{-1}) subphases for several surface pressures. The inset at the right shows evolution of band intensities for the two main bands.

the first, chitosan, with no surface activity, is anchored to the lipid surface owing to electrostatic or dipole interactions. In the second step, chitosan penetrates the monolayer, thus causing expansion. These features were well-captured in the PM-IRRAS and surface pressure measurements.

Overall, the main conclusions drawn are the following:

(a) Phosphate groups have their orientation changed by chitosan, consistent with a strong affinity between chitosan and anionic matrices.

(b) The orientation of the alkyl chains of DMPA, either in a neat monolayer or mixed with cholesterol, is affected by chitosan, which induces increased chain order.

(c) As chitosan expands the monolayer and increases chain order, a certain area of air−water interface is occupied by chitosan, which interpenetrates among the nonpolar tails.

(d) The intensity of the bands assigned to amine groups increases with monolayer compression, pointing to a higher surface density of chitosan at the interface, interpenetrating among alkyl chains or interacting with phosphate groups at the interface. Saturation of this effect occurs at 15 mN m^{-1}.

In subsidiary experiments (see the Supporting Information), we observed that chitosan affects DPPG−cholesterol monolayers much in the same way as for DMPA−cholesterol, but this is not so for the DPPC−cholesterol pair. Since DPPG is negatively charged (like DMPA) and DPPC is zwitterionic, these results reinforce the electrostatic origin of the chitosan action.

Langmuir−Blodgett (LB) Films. The effect from chitosan on mixed monolayers of DMPA and cholesterol was further investigated by transferring the Langmuir films from the air−water interface onto solid supports, thus producing Langmuir−Blodgett (LB) films. The transfer ratios of the LB films were close to 1, which confirmed the good quality of deposition. Table 1 shows the transferred mass measured with a quartz crystal microbalance (QCM). A larger mass of chitosan was transferred together with DMPA than for cholesterol, which is also attributed to the higher strength of the interaction between DMPA and chitosan. For the mixed DMPA−cholesterol film (1:1 in moles) spread on a pure buffer subphase, the deposited mass was very close to the average of the masses transferred for the pure film of each material. When mixed DMPA−cholesterol monolayers

Table 1. Mass of Material Transferred to One-Layer LB Films (Measured by Nanogravimetry) Formed by DMPA, Cholesterol, and Chitosan[a]

compound	total mass (ng)	chitosan mass (ng)
DMPA	109.5	0
DMPA−chitosan	258.2	148.8
cholesterol	70.0	0
cholesterol−chitosan	104.6	34.6
DMPA + cholesterol	90.1	0
DMPA + cholesterol−chitosan	237.5	147.4

[a] Films were transferred from a Langmuir monolayer at 40 mN m^{-1}. The chitosan concentration in the subphase was fixed at 0.20 mg mL^{-1}, and the proportion of DMPA:cholesterol was always 1:1 in moles.

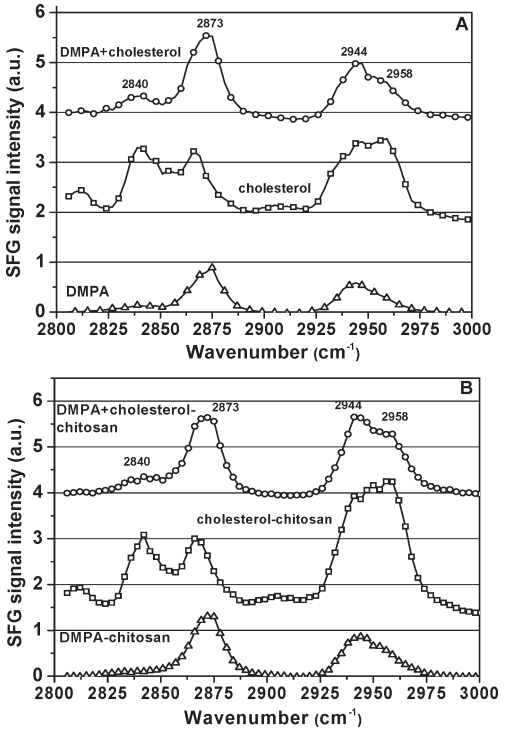

Figure 11. SFG spectra in the C−H stretch region for Langmuir−Blodgett films with DMPA, cholesterol, and chitosan, transferred at 40 mN m^{-1} from the air−water interface to infrared-grade fused silica. (A) Films of DMPA and cholesterol transferred from a chitosan-free Theorell buffer subphase. (B) Films of DMPA and cholesterol transferred from chitosan-containing (0.20 mg mL^{-1}) subphase. Mixed DMPA−cholesterol films were 1:1 in moles.

formed over chitosan-containing subphases are transferred, an amount of chitosan equivalent to that of a pure DMPA monolayer on a chitosan-containing subphase is taken to the film, 147.4 versus 148.8 ng, respectively. This means that the introduction of cholesterol at the air−water interface does not affect the chitosan transfer, i.e. the quantity of DMPA molecules at the interface is sufficient to allow for transfer of the same amount of chitosan.

The LB films were studied with sum-frequency generation (SFG) spectroscopy, which is highly sensitive to interfaces and selective to the orientation of the probed molecules.[68−70] The spectra for one-layer Langmuir−Blodgett films (in several combinations of DMPA, cholesterol, and chitosan) transferred at 40 mN m^{-1} are shown in Figure 11. For such surface pressures, a high degree of organization is expected since the monolayer is in the liquid-condensed state. It is worth noting that chitosan films, obtained by dipping fused silica supports in chitosan solution, do not display bands in the CH vibration region, because chitosan was randomly oriented on the substrate surface. Then, any influence from CH_2 groups of chitosan can be discarded.

The four main bands in the spectra with maxima at 2840, 2873, 2944, and 2958 cm^{-1} are assigned to CH_2 symmetric stretching, CH_3 symmetric stretching, CH_3 Fermi resonance, and CH_3 asymmetric stretching, respectively. The discussion will be focused on the symmetric bands because the CH_2 symmetric stretching is inactive in SFG,[46,71] unless gauche defects appear. This means the stretch intensity of this band is a direct measure for the conformational disorder in the lipid chain. On the other hand, the intensity of CH_3 symmetric stretch increases when the CH_3 groups are aligned. Therefore, the intensity of this band is a probe of the orientational order in the lipid tail.

The increase in the CH_2 symmetric stretch at ~2840 cm^{-1} for the mixed DMPA−cholesterol film compared to a pure DMPA monolayer in Figure 11 may suggest that cholesterol increases disorder of lipid chains, although it is possible that this increase could result from a contribution from CH_2 groups of cholesterol molecules. This cholesterol-induced disorder is in contrast to reports for DPPC−cholesterol mixed films where the addition of cholesterol induced ordering of alkyl chains from a disordered state (gauche defects) to all-trans bonds.[59,60] However, cholesterol has a condensing effect on DPPC monolayers which provides the ordering of alkyl chains due to increased hydrophobic interactions. For DMPA−cholesterol mixed monolayers at high surface pressures, the effect is opposite: cholesterol expands and promotes disorder of hydrophobic tails of the phospholipid. For mixed monolayers on a chitosan subphase (Figure 11B), the effect caused by cholesterol on the SFG spectrum is similar to that without chitosan. This can be better visualized in Table 2, where the ratios of the symmetric stretch intensities of CH_3 (2873 cm^{-1}) and CH_2 (2840 cm^{-1}) are displayed. For instance, cholesterol decreases the order ratio from 6.62 to 4.58 for DMPA monolayers transferred from a subphase without chitosan and from 12.91 to 5.97 for DMPA on a chitosan-containing subphase. It should be stressed that the direct influence of cholesterol over the alignment of DMPA chains cannot be inferred from the data presented here, and this requires experiments with deuterated cholesterol.

Chitosan is known to enhance the order of DMPA monolayers,[12] which can also be visualized in Table 2: the order ratio increased from 6.62 to 12.91 upon chitosan addition. The same trend is observed for mixed DMPA−cholesterol monolayers, with the order ratio increasing from 4.58 to 5.97 upon chitosan addition. For cholesterol, chitosan adsorption causes insignificant modification in the order parameter, which remains at 0.94−0.95. This confirms that the electrostatic interaction between chitosan and DMPA is the main factor promoting enhancement of the alkyl alignment.

In a previous paper,[12] we explained the ordering induced by chitosan on DMPA as being due to penetration of chitosan moieties among the hydrophobic tails of DMPA, which causes expansion of the monolayer and increases its ordering. We note that the values shown in the isotherms reflect the area occupied by lipids, disregarding possible area occupation due to the chitosan penetration. Since some chitosan moieties indeed occupy a certain area at the interface, the lipid film must be molecularly more compact, thus explaining the increase in order for the alkyl tails.

(68) Roeterdink, W. G.; Berg, O.; Bonn, M. *J. Chem. Phys.* **2004**, *121*, 10174–10180.
(69) Levy, D.; Briggman, K. A. *Langmuir* **2007**, *23*, 7155–7161.
(70) Ohe, C.; Goto, Y.; Noi, M.; Arai, M.; Kamijo, H.; Itoh, K. *J. Phys. Chem. B* **2007**, *111*, 1693–1700.
(71) Guyot-Sionnest, P. *Annal. Phys.−Paris* **1990**, *15*, 89–94.

Table 2. Ratio of SFG Intensities for the Symmetric Stretches ($v[CH_3]/v[CH_2]$) Representing Ordering of Alkyl Chains for Monolayers Formed with DMPA, Cholesterol (chol), and Chitosan (chit) Transferred from the Air−Water Interface onto Infrared-Grade Fused Silica Supports at 40 mN m^{-1}[a]

monolayer	DMPA	chol	DMPA + chol	DMPA−chit	chol−chit	DMPA + chol−chit
$v(CH_3)/v(CH_2)$	6.62	0.94	4.58	12.91	0.95	5.97

[a] The data is used as a qualitative guide to show the relative ordering of the monolayers.

Scheme 1. Summary of the Comparative Effects of Chitosan or Cholesterol to the Membrane Models Studied, for a Film Packing Close to a Real Biomembrane

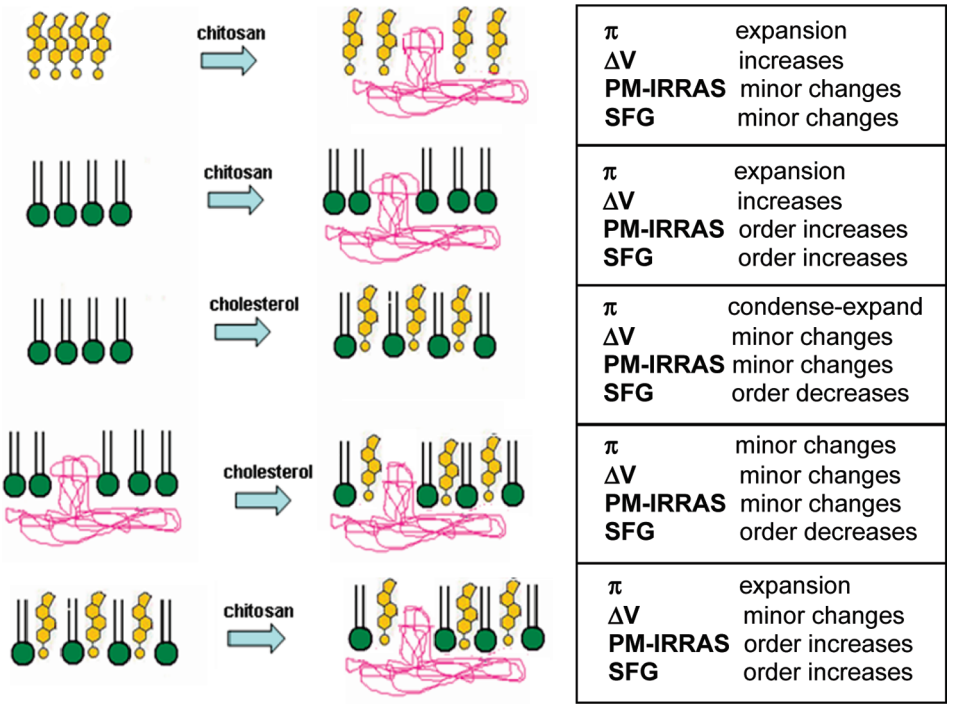

For a mixed monolayer, the order is reduced because cholesterol expands the monolayer, leaving DMPA hydrophobic tails with greater freedom to move. For mixed DMPA + cholesterol monolayers interacting with chitosan, the conformational order is again enhanced upon chitosan adsorption and penetration, in much the same way as a pure DMPA monolayer. Chitosan, therefore, is able to adsorb on all lipid layers studied: neat DMPA, neat cholesterol and mixed DMPA−cholesterol. In all cases, it expands the monolayers. For DMPA−chitosan (with or without cholesterol), the electrostatic nature of phosphate−amine interactions dominates the surface properties and induces conformational ordering of alkyl chains. In addition, using QCM measurements we have shown that both pure DMPA and mixed DMPA−cholesterol monolayers allow transfer of the same amount of chitosan.

The existence of limited points of electrostatic interaction between chitosan and DMPA may be assumed, which determines how chitosan affects the film properties. Such effects on DMPA monolayers—namely, expansion and enhancing of chain ordering—were not affected by incorporation of cholesterol. This conclusion was inferred from the combined results from SFG and QCM measurements for LB films, being supported by results for Langmuir monolayers: cholesterol does not affect the compression isotherms for DMPA monolayers on a chitosan subphase, except at very high molar percentages (80%). Furthermore, there is only a minor effect of cholesterol on the PM-IRRAS spectra of mixed DMPA−chitosan monolayers. It is therefore confirmed that electrostatic interactions are of major importance for the action of chitosan at interfaces inspired in cell membranes.

The effects from cholesterol and chitosan can be summarized in Scheme 1.

Conclusions

The fundamental role of electrostatic interactions for chitosan effects on Langmuir monolayers has been demonstrated in several instances, particularly with strong effects on negatively charged phospholipids, such as DMPA. Using PM-IRRAS for Langmuir monolayers and SFG for LB films, we showed that chitosan induces order in the alkyl chains of DMPA, while cholesterol causes disorder. Most significantly, cholesterol mediates the activity of chitosan in the monolayers and LB films of DMPA by tuning the extent of chitosan penetration. With chitosan in the subphase, cholesterol molecules occupy the same area per molecule as DMPA in mixed DMPA−cholesterol monolayers, with the final result of surface pressure isotherms being independent of the relative concentration of DMPA and cholesterol.

With regard to the biological implications, it is assumed that in many applications, such as wound healing, bactericide, and in prosthesis, the action of chitosan will depend on the interaction with lipid membranes. The results shown here point to the importance of chitosan interacting with negatively charged

regions of the membrane, with possible effects on the dissociation of ionized groups and degree of lipid lateral packing. Therefore, chitosan induces changes in local pH and in the elasticity of the membrane, in addition to the ordering of lipid and guest molecules. Furthermore, Langmuir monolayers of DMPA have a specific degree of expansion that depends strictly on the chitosan concentration and not on cholesterol quantity, which is important because cholesterol is an essential component of cell membranes. Finally, chitosan is not able to remove cholesterol from the interface, thus ruling out any hypothesis of chitosan-induced cholesterol reduction via expulsion from the membrane.

Acknowledgment. This work was supported by FAPESP, CNPq, CAPES, and Finep (Brasil). We thank KSV Instruments Ltda. for the use of the PM-IRRAS instrument.

Supporting Information Available: Figures supporting information 1−4. This material is available free of charge via the Internet at http://pubs.acs.org.